Transverse susceptibility as a probe of the magnetocrystalline anisotropy-driven phase transition in Pr_{0.5}Sr_{0.5}CoO_{3}

N. A. Frey Huls, N. S. Bingham, M. H. Phan, H. Srikanth, D. D. Stauffer, and C. Leighton

Phys. Rev. B **83**, 024406 — Published 21 January 2011

DOI: 10.1103/PhysRevB.83.024406

Transverse susceptibility as a probe of the magnetocrystalline anisotropy-driven phase transition in $Pr_{0.5}Sr_{0.5}CoO_3$

N. A. Frey Huls[1, 2], N. S. Bingham[1], M. H. Phan[1], H. Srikanth[1], D. D. Stauffer[3], and C. Leighton[3]

[1]Department of Physics, University of South Florida, Tampa, Florida 33620, USA

[2]National Institute of Standards and Technology, Gaithersburg, Maryland 20899, USA

[3]Department of Chemical Engineering and Materials Science, University of Minnesota, Minneapolis, MN 55455, USA

Half-doped $Pr_{1-x}Sr_xCoO_3$ (x=0.5) displays anomalous magnetism most notably manifest in the field-cooled magnetization versus temperature curves under different applied cooling fields. Recently, an explanation was advanced that a magnetocrystalline anisotropy transition driven by a structural transition at 120 K is the origin of this behavior. In this paper, we further elucidate the nature of the magnetic anisotropy across the low temperature phase transition in this material by means of transverse susceptibility (TS) measurements performed using a self-resonant tunnel diode oscillator. TS probes magnetic materials by means of a small radio frequency oriented transverse to a DC field which sweeps from positive to negative saturation. TS scans as a function of field clearly reveal peaks associated with the anisotropy (H_K) and switching fields (H_S). When peak position is examined as a function of temperature, around 120 K the signature of a ferromagnetic to ferromagnetic (FM-FM) phase transition is evident as a sharp feature in H_K and a corresponding cusp in H_S. A third TS peak (not previously observed in other classes of magnetic oxides such as manganites and spinel ferrites) is found to be correlated with the crossover field (H_{cr}) in the unconventional magnetization versus temperature (M(T)) behavior.

We observe a strong temperature dependence of H_{cr} around 120 K using this technique, which suggests the magnetic field-influenced magnetocrystalline anisotropy transition. We show the switching between the high-field magnetization state and the low-field magnetization state associated with the magnetocrystalline anisotropy transition is irreversible when the magnetic field is re-cycled. Finally, we demonstrate that the TS peak magnitude indicates easy axis switching associated with this phase transition, even in these polycrystalline samples. Our results further confirm that TS provides new insights into the magnetic behavior of complex oxides.

PACS: 75.30.Gw, 75.30.-m, 75.47.Lx, 75.30.Cr

Key words: Cobaltites, Magnetocrystalline anisotropy, Magnetic switching

I. INTRODUCTION

Complex oxides of the general form $Ln_{1-x}AE_xTMO_3$ (Ln= Lanthanide, AE = Alkaline-Earth, TM = Transition Metal) have drawn intense interest from the magnetism community in recent years due to their unique properties such as charge ordering [1-3], structural transitions (including the Jahn-Teller distortion [4, 5]), unusual magnetic and spin-flip transitions [6, 7], multiferroicity [8, 9], and magnetoelectronic phase separation [10, 11]. This makes them relevant in almost every area of magnetism including magnetoresistive sensors [12], spintronics (due to their high spin polarization at the Fermi surface [13, 14]), and magnetic refrigeration because of their large magnetocaloric response [15, 16].

Until recently, the discussion associated with these perovskites has been largely dominated by the manganites (TM = Mn) because they have been known to exhibit all of these

properties due to the interplay between charge, spin, lattice, and orbital degrees of freedom, which lead to multiple ground states and phase transitions [17, 18]. The relatively less-studied cobaltites (TM = Co) present interesting characteristics as well, perhaps the most well-known example being the spin-state transition in $LaCoO_3$ [19-21]. Co substituted onto the TM site leads to an additional spin-state degree of freedom due to similar magnitudes of the crystal field and Hund's rule exchange energies. This, along with the significantly larger magnetocrystalline anisotropy, makes the study of cobaltites intriguing, both for fundamental physics and device applications, where manipulation of the anisotropy is desirable.

Half-doped $Pr_{1-x}Sr_xCoO_3$ (x=0.5) is known to exhibit particularly unusual magnetic behavior that is not consistent with the phase behavior often seen in manganites and other complex oxide systems [22-26]. The field-cooled magnetization versus temperature profiles are the best example. Figure 1 shows the field-cooled magnetization versus temperature for low cooling field (1 mT, 1a) intermediate cooling field (0.1 T, 1b) and saturated cooling field (5 T, 1c). At low cooling fields the magnetization first increases with decreasing temperature and then abruptly decreases with further decrease in temperature at around 120 K (henceforth T_A). However with larger applied cooling fields, the magnetization first increases with decreasing temperature and then increases even more sharply at temperatures lower than T_A. The field-dependent M(T) behavior crosses over from decreasing below T_A to increasing below T_A at a field of around 75 mT, which we will refer to as H_{cr}. At cooling fields in which the magnetization is saturated, no anomaly is observed in the M(T). Note that the decrease (increase) in magnetization upon cooling in low (high) field is manifest as a gradual change in curvature starting at around T_A and persists well into the low temperature regime.

In order to understand this apparently paradoxical behavior, systematic studies were recently undertaken to rule out the phase transitions most routinely associated with perovskites such as charge ordering, antiferromagnetic ordering, ferrimagnetism, or spin-flip transitions [27]. It was conclusively shown that all the observed behavior can be explained by a ferromagnetic to ferromagnetic (FM-FM) transition resulting from a structural change which drives a transition in the magnetocrystalline anisotropy. Interestingly, this structural transition does not appear to cause a change in crystal symmetry. Our team has previously reported that both above and below T_A, $Pr_{0.5}Sr_{0.5}CoO_3$ is monoclinic with space group $I2/a$ and the overall volume of the unit cell remains largely unaltered [27], though other recent findings have been somewhat contradictory [28] . We find that the *a* and *b* lattice parameters undergo significant changes of +1.15 % and -1.10 % respectively upon cooling through the 120 K transition, which alters the spin-orbit coupling and thus appears as a transition in the magnetocrystalline anisotropy. The result is two ferromagnetic phases consisting of a lower anisotropy phase (labeled FM1) at low temperature (below T_A) and a higher anisotropy phase (labeled FM2) at intermediate temperatures between T_A and T_C ($T_C \approx 230$ K for $Pr_{0.5}Sr_{0.5}CoO_3$). Since each of the two phases has distinct anisotropy features, a detailed study of magnetic anisotropy and its manifestation in the field and temperature dependence is of critical importance, which is the focus of the results presented in this paper. In addition, it would be very interesting to study if the switching between the high-field magnetization state (Fig. 1b) and the low-field magnetization state (Fig. 1a) associated with the magnetocrystalline anisotropy transition is reversible when the magnetic field is swept between zero and high field.

Because this FM-FM transition is not seen in transport measurements, and traditional magnetometry measurements shed limited light on the nature of the magnetocrystalline anisotropy, we assert that the transverse susceptibility (TS) measurement technique – a reliable direct probe of the anisotropy and switching fields of a material – is extremely well-suited to explore this particular structure-driven magnetocrystalline anisotropy transition. Besides the drastic change in magnitude of the anisotropy of $Pr_{0.5}Sr_{0.5}CoO_3$ across T_A directly probed by TS experiments, we reveal a clear temperature dependence of H_{cr} around T_A using this technique. We show the irreversible switching between the high-field magnetization state and the low-field magnetization state, associated with the magnetocrystalline anisotropy transition, when the magnetic field is re-cycled. We also show that the changing magnitude of the directional- and field-dependent susceptibilities (H_{AC} perpendicular to H_{DC} and H_{AC} parallel to H_{DC}) also reveal the change in *direction* of the anisotropy. This is fully consistent with Lorentz microscopy [24] and traditional magnetometry [25] studies on single crystals of $Pr_{0.5}Sr_{0.5}CoO_3$ showing that there is a change in direction of the anisotropy vector with the easy axis of magnetization rotating from [110] at higher temperatures to [100] at low temperature.

II. EXPERIMENTAL DETAILS

Bulk polycrystalline samples of $Pr_{0.5}Sr_{0.5}CoO_3$ were synthesized according to the procedure outlined in reference [27]. In short, stoichiometric quantities of Pr_2O_3, $SrCO_3$, and Co_3O_4 were reacted at 1000 °C for 7 days with several intermediate grindings followed by cold pressing, sintering at 1200 °C for 1 day, and slow cooling (1 °C/min) to room temperature. Thermogravimetric analysis revealed there were approximately 0.1 missing oxygen atoms per

unit cell at this doping level and oxygen deficiency has been ruled out as an explanation for the magnetic anomalies observed for all the doping ranges studied in our collaboration. Extensive structural analysis, transport measurements and magnetic property measurements were also carried out and discussed in reference [27].

Transverse susceptibility measurements were performed using a self-resonant tunnel diode oscillator with a resonant frequency of 12 MHz and sensitivity on the order of 10 Hz [29]. The tunnel diode oscillator is housed outside of a commercial Physical Properties Measurement System (PPMS, Quantum Design [30]) which serves to modulate the applied DC magnetic field ($\mu_0 H$ up to ±7 T) as well as the measurement temperature (2 K < T < 300 K). The sample is placed in the inductance coil of the tank circuit which is integrated into the PPMS such that the perturbing RF magnetic field inside the coil ($\mu_0 H_{AC} \approx 1$ mT) is oriented perpendicular to the superconducting magnet. The transverse susceptibility (TS) measurement for a given temperature is performed by monitoring the change in the resonant frequency of the circuit as the DC field is swept from positive saturation to negative saturation and then back to positive (bipolar scan). Because the change in frequency of the circuit is a direct consequence of the change in inductance as the sample is magnetized, the quantity Δf is directly proportional to $\Delta \chi_T$. We are therefore most interested in the quantity

$$\frac{\Delta \chi_T}{\chi_T}(\%) = \frac{|\chi_T(H) - \chi_T^{sat}|}{\chi_T^{sat}} \times 100$$

as a function of H_{DC} where χ_T^{sat} is the transverse susceptibility at the saturating field H_{sat}. In accordance with Aharoni *et al.*'s theoretical predictions [31], as well as other TS models [32,33], we observe maxima in the TS scan at the positive and negative anisotropy fields of the material, $\pm H_K$, and at the switching field, H_S, for a unipolar sweep of the DC field from positive to negative saturation. This technique has been used with great success to examine the anisotropic magnetic properties of a variety of systems from multilayered thin films [34] to single crystals [35] and nanoparticles [36, 37]. However it also lends itself particularly well to the rich physics involved in complex oxide systems to examine the unusual magnetic behavior often seen in manganites [28, 32, 35, 39] and, as we show here, cobaltites.

III. RESULTS AND DISCUSSION

TS measurements were performed on a polycrystalline $Pr_{0.5}Sr_{0.5}CoO_3$ sample (approximately 12 mm x 6 mm x 4 mm) at a number of temperatures to examine the temperature dependence of the anisotropic features across the 120 K transition. Figure 2 shows bipolar TS scans of $Pr_{0.5}Sr_{0.5}CoO_3$ taken at four representative temperatures: 20 K (2a), 95 K (2b), 110 K (2c), and 225 K (2d). Arrows have been inserted into figure 2c to indicate the sequence of measurement, and the peaks discussed below have been labeled in figure 2a. The broader, high-field peaks seen on either side of $\mu_0 H=0$, closest to saturation, are the anisotropy peaks indicating the anisotropy fields, $\pm H_K$. The broad nature of the anisotropy peak can be ascribed to dispersion in the anisotropy axes in polycrystalline samples. Frequently, in physical systems that deviate from the theoretical conditions outlined in TS models and predictions, the H_K peaks are not located symmetrically about $\mu_0 H = 0$, differing both in magnitude and applied field value (i.e.

$+H_K \neq -H_K$). In all such cases $-H_K$ is smaller in magnitude but occurs at higher field and is often broader in comparison to the $+H_K$ peak. This phenomenon is the subject of a previous study [37], and it is largely accepted that the differences in shape and placement of the $-H_K$ peak relative to the $+H_K$ peak in particulate systems is heavily dependent on such factors as inter-particle interactions, both dipolar and exchange in nature, as well as anisotropy and switching field distributions. A brief explanation for this is that the first anisotropy peak occurring after saturation arises under a different free-energy landscape than the second peak, which occurs after decreasing $\mu_0 H$ past the switching and coercive fields, but before saturation in the opposite direction. For this reason, we consistently use $+H_K$ when referring to the anisotropy field.

In the case of $Pr_{0.5}Sr_{0.5}CoO_3$, the $-H_K$ peak changes in shape over the temperature range studied; at low temperatures it is so smeared out as to be nearly impossible to determine its value. While we cannot make a direct comparison to the case of the particulate systems studied in reference [37], we note that, analogous to interacting nanoparticle systems, polycrystalline samples experience inter-granular exchange interactions and different magnetic environments upon reaching saturation and subsequently passing through the coercive field, thus affecting the shape and magnitude of the $-H_K$ peak. In fact it has been observed [27] that the small low temperature magnetic susceptibility seen in the magnetizing (M-H) curves of this system is indicative of poor magnetic coupling between grains, which is also very consistent with the $-H_K$ shape observed in only weakly-interacting particulate systems.

The second peak is only observed upon decreasing the field after positive (or negative) saturation. The presence of this peak lends insight to the crossover behavior between the two

types of anomalous M(T) curves. We attribute this peak to the "crossover field", H_{cr} which separates the lower field-cooled magnetization state from the higher field-cooled magnetization state for any given temperature occurring in the vicinity of the FM-FM transition. The origin of H_{cr} and its temperature dependence will be discussed in detail below.

The third peak observed is the prominent switching peak, H_S. It is important to note that in the transverse susceptibility set-up, the signal is dominated by those crystallites whose easy axes of magnetization are perpendicular to the bias DC field. Therefore, the switching peak is not correlated simply with the maximum of the derivative of the M-H curve (as is the case for the parallel susceptibility measurement), which is a collective response contributed to by all crystallites. The parallel susceptibility measurement, (in which $H_{AC} \parallel H_{DC}$), does give the switching field as averaged over the entire sample. The peaks observed under the two different geometries therefore will not generally occur at the same field in polycrystalline samples.

Now that the peaks present have been identified, let us focus on the trends observed for the basic shape of the TS profile at the representative temperatures. The TS scans at 20 K (figure 2a) and 95 K (figure 2b) are fully consistent with other systems upon increasing the temperature. The anisotropy, switching, and crossover field peaks are sharp and well-defined at 20 K. At 95 K, the features become slightly more ambiguous and the curve becomes narrower in shape as the anisotropy features are shifted to lower fields. Figures 2a through 2d have the same x-axis scale so it is easy to see that the overall TS profile has become narrower with increasing temperature. This evolution from wide, sharp features to narrower, smaller features has been seen numerous times in TS studies of materials as their Curie temperature is approached [34-37]. However, this

trend does not continue as the temperature increases across T_A, as it would if it were approaching a phase transition from, for example, an FM to a paramagnetic state. Although the structural transition has significant width (as evidenced by the M(T) curves), by 110 K (figure 2c) the TS curve has taken on a dramatically different shape than that seen at 95 K. The peaks are once again very well-defined with features occurring at higher fields than even at lower temperatures. By 225 K (figure 2d) the curve is once again narrower as the material approaches its Curie temperature (230 K). It is interesting to note that by 225 K the peak associated with the crossover field is gone, as the material has now entered the regime, seen in the M(T) curves, where the behavior is the same regardless of the cooling field.

To better illustrate the difference in anisotropy features between FM1 and FM2, we have superimposed the TS curves for each phase onto two separate plots. Figure 3a shows the temperature evolution of the TS curves for phase FM1 and figure 3b shows the temperature evolution of the TS curves for FM2. Unlike in figure 2, the magnitude of the TS signal appears in arbitrary units so that all the curves could be fit onto either graph in a manner that still clearly shows the important features. What is remarkable is the degree to which the two phases differ in appearance. Whereas FM1 has a very well-defined $+H_K$ peak for all temperatures up to the transition, and displays the crossover field peak, the FM2 curve is largely dominated by the intense switching peak. The anisotropy peak appears much broader. We note here that while the TS experiments reveal clear differences in anisotropy features between FM1 and FM2, this picture remains slightly ambiguous in the M(T) and M(H) data. The relative appearance of the curves for FM1 and FM2 is akin to the comparison of two different materials entirely, rather than

the comparison of two structural phases of the same material. This once again indicates that the TS technique is more suitable for studying anisotropy-driven transitions.

The differences in anisotropy peak, switching peak, and crossover field peak across the transition at T_A are quantitatively examined in figure 4, where we present the field associated with each of these peaks as a function of temperature. Figure 4a shows the anisotropy field ($+H_K$) as a function of temperature where it is conclusively demonstrated that the FM2 phase of $Pr_{0.5}Sr_{0.5}CoO_3$ has a higher magnetocrystalline anisotropy than the lower temperature, FM1 phase. For lower temperatures ($T < T_A$,) the anisotropy field decreases with increasing temperature, which is typical of most magnetic systems as the thermal energy begins to compete with the anisotropy energy of the system. The structural transition at 120 K then appears as a dramatic increase in anisotropy field to values even higher than those seen at the lowest temperatures – $\mu_0 H_K \approx 184$ mT at 120 K versus ≈125 mT at 10 K. The sharp change in H_K at T_A is a direct consequence of the coupled structural/magnetocrystalline anisotropy transition, which was hypothesized to involve the effects of Pr-O bonding [27]. After reaching this maximum, H_K then slowly decreases again until T_C where it goes to zero. The decrease of H_K with temperature for $T < T_A$ and for $T_A < T < T_C$ is fully consistent with the perspective that the $Pr_{0.5}Sr_{0.5}CoO_3$ system undergoes a transition from one FM state to another.

The switching field (H_S) is tracked as a function of temperature in figure 4b. Its shape closely follows that reported in reference [27] (not shown) for both the coercivity and fraction of irreversible magnetization as measured by the first order reversal curve method [40]. This is not surprising as all three properties are direct consequences of irreversible hysteretic processes. At

low temperatures it decreases rapidly until the approach to T_A where it experiences an increase and a cusp at 120 K, and then decreases again until T_C.

Figure 4c shows the evolution of the peak position associated with the crossover field (H_{cr}) as a function of temperature. In the introduction section, it was briefly stated that the cooling field required to change the shape of the temperature dependent magnetization curve from the drop in magnetization (figure 1a) to the increase in magnetization (figure 1b) roughly corresponds to 75 mT. This feature has been observed in the field-cooled regime but not in the zero-field-cooled one [27]. This can be reconciled with the TS data (figure 2) that indicate that the second peak corresponding to H_{cr} is only observed upon decreasing the field after positive (or negative) saturation, not upon increasing the field from zero field. It is worth noting from TS experiments that for a given temperature, when the magnetic field is decreased from saturation field (1 T) to zero field, TS reflects the two entirely different magnetization states. In the field range $H_{cr} < H < 1$ T, TS reflects the magnetization state similar to that seen in figure 1b, while for $H < H_{cr}$ TS reflects the magnetization state similar to that seen in figure 1a. While the temperature dependence of H_{cr} is not visibly revealed from the M(T) and M(H) data (in fact no corresponding H_{cr} feature is seen at all in M(H)) , TS experiments reveal a clear temperature dependence of H_{cr} below T_A. Since transverse susceptibility is a measure of the field-derivative of the magnetization, it is unsurprising that subtle changes in M(T) or M(H) should show up as well-defined peaks in this measurement, again indicating that TS is ideal for investigating unusual features in magnetic anisotropy that are not often picked up clearly in conventional magnetometry. This is consistent with the previous observation by Patanjali et al. [38] that revealed via TS experiments the existence of a new, secondary transition at high temperature in a

double perovskite $La_{1.2}Sr_{1.8}Mn_2O_7$, which was not observed by static resistivity and magnetization measurements. In the case of $Pr_{0.5}Sr_{0.5}CoO_3$, the largest H_{cr} is indeed measured by TS to be 75 mT around T_A (figure 4c), which coincides with that deduced from the M(T) data (figure 1). However, at lower temperatures, the change in shape of the magnetization curves appears to occur at much lower fields, around 20 mT. The crossover field increases gradually with temperature up to 75 K - the onset temperature of the FM-FM transition and then increases rapidly with temperature up to T_A. This crossover field does go to zero shortly after the FM-FM transition, which corresponds to the region where the M(T) curves display qualitatively identical behavior no matter the cooling field. It has been noted that due to poor magnetic coupling between the grains at low temperatures ($T << T_A$), the initial susceptibility is smaller in the FM1 region than in the FM2 regions [27]. In addition, we find that the magnetization increases with increasing temperature in the FM1 region below the crossover field (see figure 5). Therefore, the increase of H_{cr} with temperature at $T < T_A$ revealed in the TS profile is as expected, consistently pointing to thermally activated improvement in intergranular coupling in this temperature range. The strong temperature dependence of H_{cr} around T_A suggests that the magnetocrystalline anisotropy transition is not only driven by the structural change but also by the magnetic field. The magnetic field- and temperature-induced magnetocrystalline anisotropy transition has been reported in $Gd_5(Si_xGe_{1-x})_4$ ($0.24 < x < 0.5$) materials [41]. Unlike in the case of $Pr_{0.5}Sr_{0.5}CoO_3$, however, this magnetocrystalline anisotropy transition is a first-order ferromagnetic to paramagnetic transition accompanied by a structural transition (from orthorhombic to monoclinic). As a result, the larger magnetic fields are needed to drive the paramagnetic/monoclinic phase to the ferromagnetic/orthorhombic one for the case of

$Gd_5(Si_xGe_{1-x})_4$ ($0.24 < x < 0.5$) materials [41]. Another important consequence that emerges from the TS data (figure 2) is that the TS peak corresponding to H_{cr} is only observed upon decreasing the field after positive (or negative) saturation but not upon increasing the field from zero field. This observation provides clear evidence that the switching between the high-field magnetization state and the low-field magnetization state around T_A in $Pr_{0.5}Sr_{0.5}CoO_3$ is irreversible, when the magnetic field is re-cycled.

In figure 6a we have plotted the magnitude of the susceptibility signal for the switching peak as a function of temperature. The solid squares are for the transverse susceptibility scans where the phase transition at 120 K can be clearly seen as a local minimum between the two phases. The open circles are data points taken of the switching peak using the parallel susceptibility (PS) method, where $H_{AC} \parallel H_{DC}$. This measurement is performed by simply rotating the coil that goes inside the magnet by 90°, so neither the circuit configuration nor the sample position within the coil has changed. The temperature dependence of the TS and PS magnitude consistently follows that of the ac susceptibility (figure 6b) showing two maxima in $\chi'(T)$ at T_C and at 75 K (the onset temperature of the FM-FM transition). The transition at 120 K can be clearly seen as a local minimum between the two phases. While the frequency independence of the $\chi'(T)$ peaks revealed from ac susceptibility measurements (figure 6b) suggests $Pr_{0.5}Sr_{0.5}CoO_3$ undergoes a PM-FM transition at $T_C \sim 230$ K followed by the FM-FM transition at $T_A \sim 120$ K, the distinguishable difference in the magnitude between TS and PS in the FM1 and FM2 ranges (figure 6a) is noteworthy. As previously mentioned, the signal from the transverse susceptibility is dominated by those crystallites in the sample whose hard axes are aligned with the DC magnetic field. The parallel susceptibility measurement, basically the derivative of the M-H

curve, has a signal essentially averaged over all orientations. It can be seen in figure 6a that for FM1 (low temperature phase) the magnitude of the signal obtained in the parallel configuration is larger than that obtained in the transverse configuration. This would imply that while there is significant signal from crystallites with the easy axis 90° from H_{DC}, the overall magnetic susceptibility is dominated by crystallites with their easy axes at angles other than 90° to H_{DC}. However, after the transition, while the signal from both orientations increases to that above the previous maximum, now the situation is reversed. The signal is much stronger coming from the crystallites with their hard axes along H_{DC} than the average switching peak orientation.

This "crossover" behavior (not to be confused with H_{cr}) tells us two things about the sample studied: (1) there is some preferred orientation of grains within the sample, otherwise the *relative* contribution to the susceptibility (i.e. the space between the parallel and transverse susceptibility curves) should stay the same across the transition and (2) this preferred orientation actually changes direction across the transition resulting in a much higher transverse susceptibility signal in the FM2 phase. While the sample has a polycrystalline nature, the fact that there is a slight preference for grain growth along one direction can be understood given the shape anisotropy of the sample, especially since the sample was measured with the long axis perpendicular to H_{DC}. This is consistent with the easy magnetic axis of the higher temperature ferromagnetic phase (FM2) growing slightly preferentially along the long dimension of the sample. Such texturing does not have to be a large effect to be clearly seen in a transverse susceptibility measurement [42]. But it is important to note that even while this preferred grain orientation along with the shape anisotropy of the sample can easily explain why TS > PS in FM2, it cannot explain the crossover that occurs across the transition. The switch from TS > PS

to TS < PS with decreasing temperature can only occur if the anisotropy vector changes direction as well as magnitude, due to the transition in a- and b-axis lattice parameters [27]. This is consistent with the previous observations using Lorentz microscopy [24] and traditional magnetometry [25] on single crystals of $Pr_{0.5}Sr_{0.5}CoO_3$ that indicate that a change in direction of the anisotropy vector occurs with the easy axis of magnetization rotating from [110] at higher temperatures to [100] at low temperature. Hwoever, even though we demonstrate that this method can tell us the change in anisotropy direction by ruling out other contributions that do not change with experimental geometry, we cannot use these results to gain further information as to the crystallographic structure of this material before or after the magnetocrystalline anisotropy transition. While TS has been used in the past to observe similar reorientation of magnetization axis in Cr_2O_3/CrO_2 bilayer thin films [34], this represents the first time TS has been used to observe the rotation of anisotropy axis in a polycrystalline sample.

IV. CONCLUSIONS

We have used the transverse susceptibility measurement technique to examine the anisotropic magnetic properties of $Pr_{0.5}Sr_{0.5}CoO_3$, specifically the structure-driven magnetocrystalline anisotropy transition at 120 K. We were able to show using this technique that the FM-FM phase transition is clearly manifest in the evolution of the anisotropy and switching peaks with temperature. The well-documented unusual M(T) behavior, dependent upon cooling field, is present in the TS as well in the form of a sharp peak at the crossover field which disappears above T_A. That this crossover field – only present upon demagnetizing after saturation – has a significant magnetic-field dependence suggests the structural transition is also

influenced by magnetic field. Its absence upon magnetizing implies the switching from high-field to low-field magnetization state is irreversible with field cycling. Lastly, we showed that the rotation of the easy axis can also be deduced by comparing the signal intensity from two different measurement orientations where a crossover behavior is observed. Collectively these findings show that transverse susceptibility is a very useful method for lending insight into the unusual magnetic behavior of doped perovskites.

ACKNOWLEDGEMENTS

Work at USF is supported by the Department of Energy through Grant No. DE-FG02-07ER46438. Work at UMN was supported by the NSF (sample synthesis) and DoE (neutron scattering characterization), via grant numbers DMR-0804432 and DE-FG02-06ER46275.

REFERENCES

[1] Y. Tomioka, A. Asamitsu, Y. Moritomo, H. Kuahara, and Y. Tokura, Phys. Rev. Lett. **74**, 5108 (1995).

[2] Y. Tokura and N. Nagaosa, Science 288, 462 (2000).

[3] E. Dagotto, Science 309, 257 (2005).

[4] A. J. Millis, P. B. Littlewood, and B. I. Shraiman, Phys. Rev. Lett. **74**, 5144 (1995).

[5] E. K. Abdel-Khalek, A. F. Salem, E. A. Mohamed, and A. A. Bahgat, J. Magn. Magn. Mater. **322**, 909 (2010).

[6] H. Kawano, R. Kajimoto, H. Yoshizawa, Y. Tomioka, H. Kuwahara, and Y. Tokura, Phys. Rev. Lett. **78**, 4253 (1996).

[7] Z. Q. Li, X. H. Zhang, H. Liu, X. D. Liu, W. B. Mi, H. L. Bai, X. N. Jing, and E. Y. Jiang, Sol. St. Comm. **130**, 563 (2004).

[8] S. W. Cheong and M. Mostovoy, Nat. Mater. **6**, 13 (2007).

[9] D. I. Khomskii, J. Magn. Magn. Mater. **306**, 1 (2006).

[10] E. Dagotto, Nanoscale Phase Separation and Colossal Magnetoresistance (Springer, New York, 2002).

[11] S. Cao, B. Kang, J. Zhang, and S. Yuan, Appl. Phys. Lett. **88**, 172503 (2006).

[12] P. Schiffer, A. P. Ramirez, W. Bao, and S.-W. Cheong, Phys. Rev. Lett. **75**, 3336 (1995).

[13] Y. Ji, C. L. Chien, Y. Tomioka, and Y. Tokura, Phys. Rev. B **66**, 012410 (2002).

[14] B. Nadgorny, I. I. Mazin, M. Osofsky, R. J. Soulen, Jr., P. Broussard, R. M. Stroud, D. J. Singh, V. G. Harris, A. Arsenov, and Ya. Mukavskii, Phys. Rev. B **63**, 184433 (2001).

[15] M.-H. Phan and S.-C. Yu, J. Magn. Magn. Mater. **308**, 325 (2007).

[16] N. S. Bingham, M.-H. Phan, H. Srikanth, M. A. Torija, and C. Leighton, J. Appl. Phys. **106**, 023909 (2009).

[17] C. N. R. Rao and B. Raveau (Editors), Colossal Magnetoresistance, Charge Ordering and Related Properties of Manganese Oxides World Scientific, Singapore (1998); *Colossal Magnetoresistance Oxides,* edited by Y. Tokura, Monographs in Condensed Matter Science (Gordon and Breach, New York, 1999).

[18] V. B Shenoy and C.N.R Rao, Phil. Trans. R Soc. A 366, 63 (2008) J. M. D. Coey, M. Viret, and S. von Molnár, Adv. Phys. **48**, 167 (1999).

[19] A. Podlesnyak, S. Streule, J. Mesot, M. Medarde, E. Pomjakushina, K. Conder, A. Tanaka, M. W. Haverkert, and D. I. Khomskii, Phys. Rev. Lett. **97**, 247208 (2006).

[20] D. P. Kozlenko, N. O. Golosova, Z. Jirák, L. S. Dubrovinsky, B. N. Savenko, M. G. Tucker, Y. Le Godec, and V. P. Glazkov, Phys. Rev. B **75**, 064422 (2007).

[21] R. F. Kile, J. C. Zheng, Y. Zhu, M. Varela, J. Wu, and C. Leighton, Phys. Rev. Lett. **99**, 047203 (2007).

[22] K. Yoshii, A. Nakamura, H. Abe, M. Mizumaki, and T. Muro, J. Magn. Magn. Mater. **239**, 85 (2002).

[23] R. Mahendiran and P. Schiffer, Phys. Rev. B **68**, 024427 (2003).

[24] M. Uchida, R. Mahendiran, Y. Tomioka, Y. Matsui, and K. Ishizuka, Appl. Phys. Lett. **86**, 131913 (2005).

[25] S. Hirahara, Y. Nakai, K. Miyoshi, K. Fujiwara, and J. Takeuchi, J. Magn. Magn. Mater. **310**, 1866 (2007).

[26] M. Patra, S. Majumdar, and S. Giri, J. Appl. Phys. **107**, 033912 (2010).

[27] C. Leighton, D. D. Stauffer, Q. Huang, Y. Ren, S. El-Khatib, M. A. Torija, J. Wu, J. W. Lynn, L. Wang, N. A. Frey, H. Srikanth, J. E. Davies, K. Liu, and J. F. Mitchell, Phys. Rev. B **79**, 214420 (2009).

[28] A. M. Balagurov, I. A. Bobrikov, D. V. Karpinsky, I. O. Troyanchuk, V. Yu. Pomjakusin, and D. V. Sheptyakov, JETP Lett., **88**, 531 (2008).

[29] H. Srikanth, J. Wiggins, and H. Rees, Rev. Sci. Instrum. **70**, 3097 (1999).

[30] We identify certain commercial equipment, instruments, or materials in this article to specify adequately the experimental procedure. In no case does such identification imply recommendation or endorsement by the National Institute of Standards and Technology, nor does it imply that the materials or equipment identified are necessarily the best available for the purpose.

[31] A. Aharoni, E. H. Frei, S. Shtrikman, and D. Treves, Bull. Res. Counc. Isr., Sect. F **6A**, 215 (1957).

[32] D. Cimpoesu, A. Stancu, and L. Spinu, Phys. Rev. B, **76**, 054409 (2007).

[33] A. Stancu and L. Spinu, J. Magn. Magn. Mater., **266**, 200 (2003).

[34] N. A. Frey, S. Srinath, H. Srikanth, M. Varela, S. Pennycook, G. X. Miao, and A. Gupta, Phys. Rev. B **74**, 024420 (2006).

[35] G. T. Woods, P. Poddar, H. Srikanth, and Ya. M. Mukovskii, J. Appl. Phys. **97**, 10C104 (2005).

[36] R. Swaminatham, M. E. McHenry, P. Poddar, and H. Srikanth, J. Appl. Phys. **97**, 10G104 (2005).

[37] P. Poddar, M. B. Morales, N. A. Frey, S. A. Morrison, E. E. Carpenter, and H. Srikanth, J. Appl. Phys. **104**, 063901 (2008).

[38] P. V. Patanjali, P. Theule, Z. Zhai, N. Hakim, S. Sridhar, R. Suryanarayanan, M. Apostu, G. Dhalenne, A. Revcolevschi, Phys. Rev. B 60, 9268 (1999).

[39] V. B. Naik and R. Mahendiran, Appl. Phys. Lett. **94**, 142505 (2009).

[40] C. R. Pike, Phys. Rev. B **68**, 104424 (2003).

[41] E. M. Levin, A. O. Pecharsky, V. K. Pecharsky, and K. A. Gschneidner, Jr. Phys. Rev. B 63, 064426 (2001).

[42] P. M. Sollis, P. R. Bissell, and R.W. Chantrell, J. Magn. Magn. Mater. **155**, 123 (1996).

FIGURE CAPTIONS

FIG. 1. Magnetization versus temperature measured upon cooling for several applied fields. (a) $\mu_0 H$= 1 mT where there is a decrease in magnetization with decrease in temperature below 120 K. (b) $\mu_0 H$ = 0.1 T where there is an increase in magnetization with decrease in temperature. The 120K anomaly is visible. (c) $\mu_0 H$ = 5 T where no anomaly can be detected.

FIG. 2. Bipolar transverse susceptibility scans of $Pr_{0.5}Sr_{0.5}CoO_3$ as a function of applied field for 20 K (a), 95 K (b), 110 K (c), and 225 K (d). On 2(a) the arrows indicate the sequence of measurement and the anisotropy (H_K), crossover (H_{cr}), and switching (H_S) peaks are labeled.

FIG. 3. Unipolar transverse susceptibility scans for several different temperature plotted on two plots depicting the two different ferromagnetic phases ((a) is FM1 and (b) is FM2). The signal intensity appears in arbitrary units as soon of the curves have been shifted upward or downward for clarity.

FIG. 4. Temperature dependence of the peaks positions in the transverse susceptibility measurement. (a) Anisotropy field ($+H_K$) position versus temperature. (b) Switching field (H_S) position versus temperature. (c) Crossover field (H_{cr}) position versus temperature. All three graphs show local maxima at the 120 K transition.

FIG. 5. Magnetizing curves for $Pr_{0.5}Sr_{0.5}CoO_3$ taken at four different temperatures showing distinct behavior upon approach to saturation before (10 K, 30 K, 60 K) and after (120 K) the FM-FM transition.

FIG. 6. (a) Switching field peak intensity $(\Delta\chi/\chi)_{max}$ as a function of temperature taken using two different geometries. The open circles are from parallel susceptibility scans and the solid circles are from transverse susceptibility scans. That the relative signal intensities undergo a crossover

around the transition temperature is an indication that the anisotropy axis rotates during the structural transition. (b) Real part of the ac susceptibility scan as a function of temperature reveals a small, frequency independent peak around 120 K signaling the FM1-FM2 transition and a larger, sharper peak at the Curie temperature. The relative peak heights of the two phases clearly mimics the field dependent susceptibility curves in 6a.

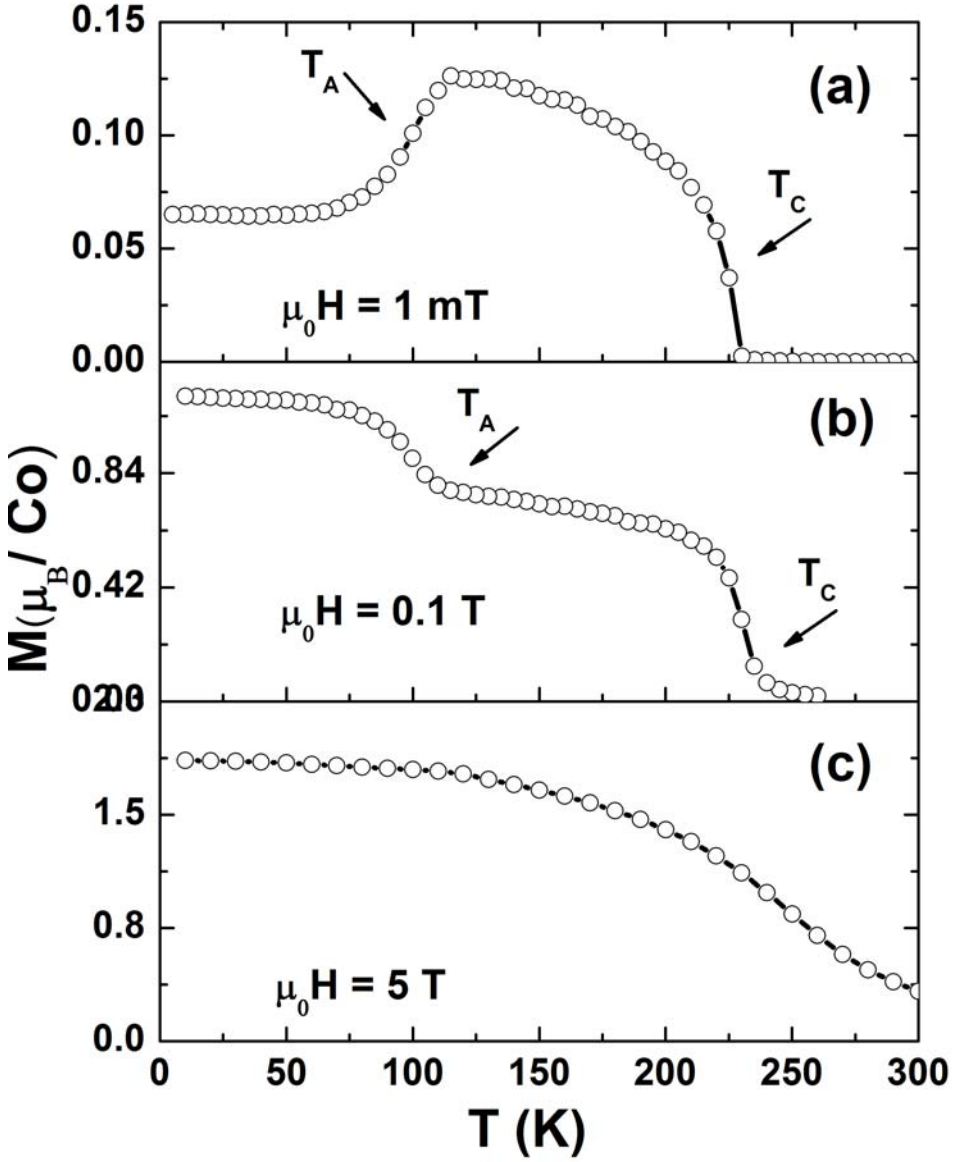
0.15
0.10
0.05
0.00
T_A
(a)
T_C
μ0H = 1 mT
T_A
(b)
0.84
0.42
T_C
μ0H = 0.1 T
(c)
1.5
0.8
0.0
μ0H = 5 T
M(μB / Co)
0
50
100
150
200
250
300
T (K)

Figure 1.

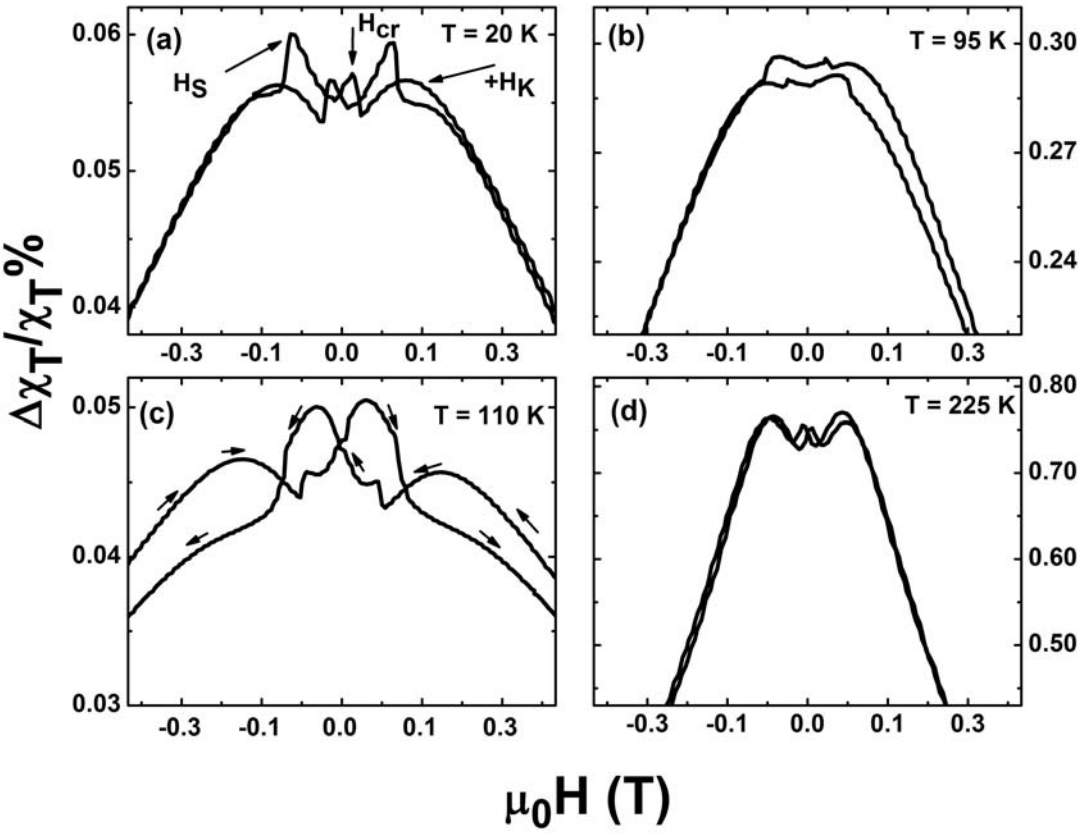

Figure 2.

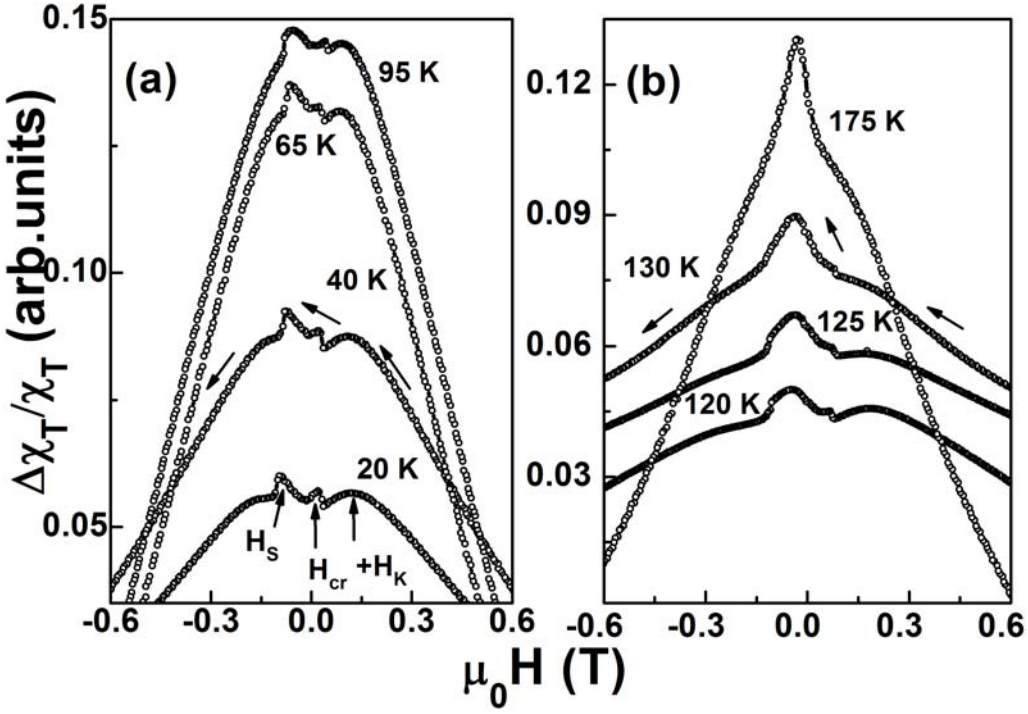
0.15
0.10
0.05
(a)
95 K
65 K
40 K
20 K
H_S
H_{cr}
$+H_K$
$\Delta\chi_T/\chi_T$ (arb.units)
-0.6
-0.3
0.0
0.3
0.6
0.12
0.09
0.06
0.03
(b)
175 K
130 K
125 K
120 K
$\mu_0 H$ (T)

Figure 3.

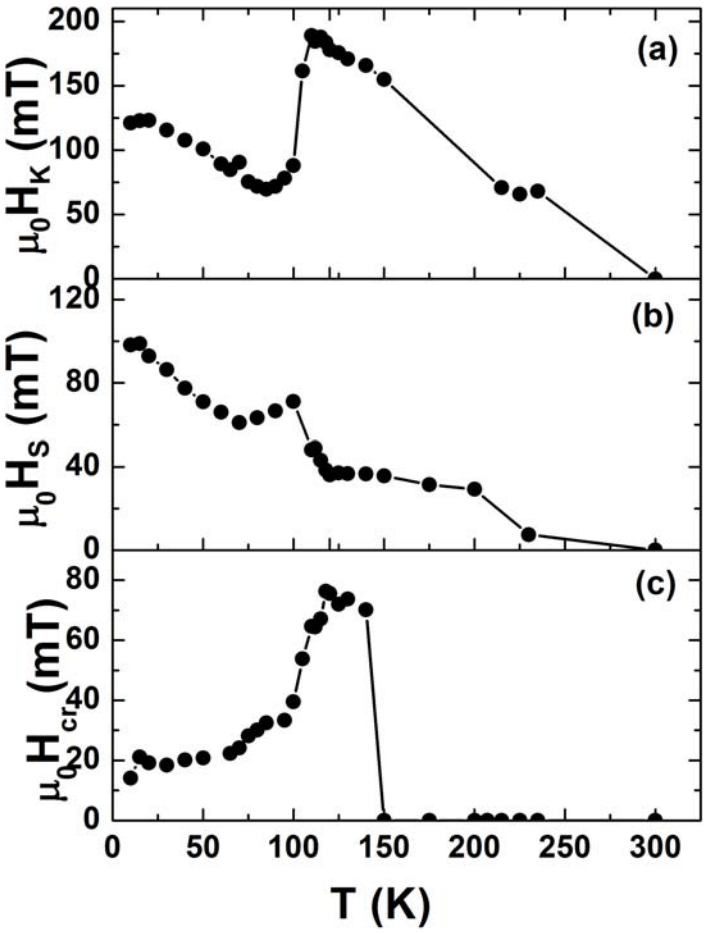
(a)
(b)
(c)
$\mu_0 H_K$ (mT)
$\mu_0 H_S$ (mT)
$\mu_0 H_{cr}$ (mT)
T (K)
0
50
100
150
200
250
300
0
40
80
120
0
20
40
60
80
0
50
100
150
200

Figure 4.

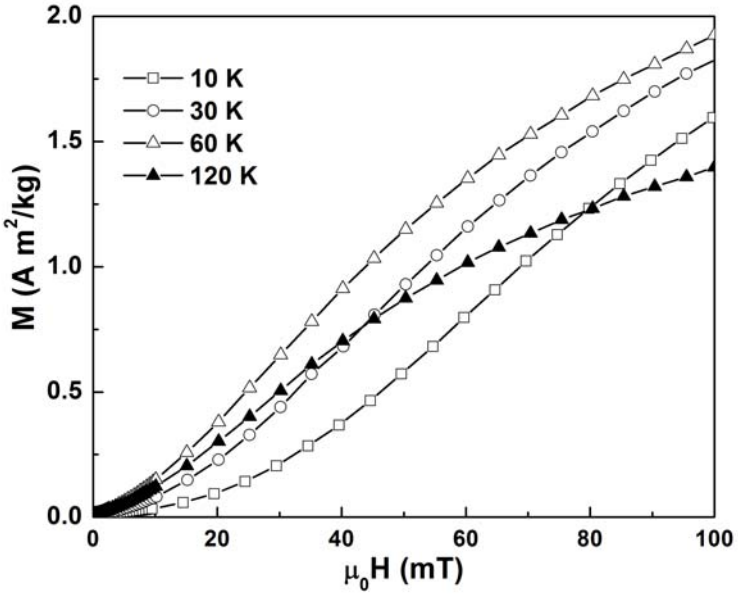

Figure 5.

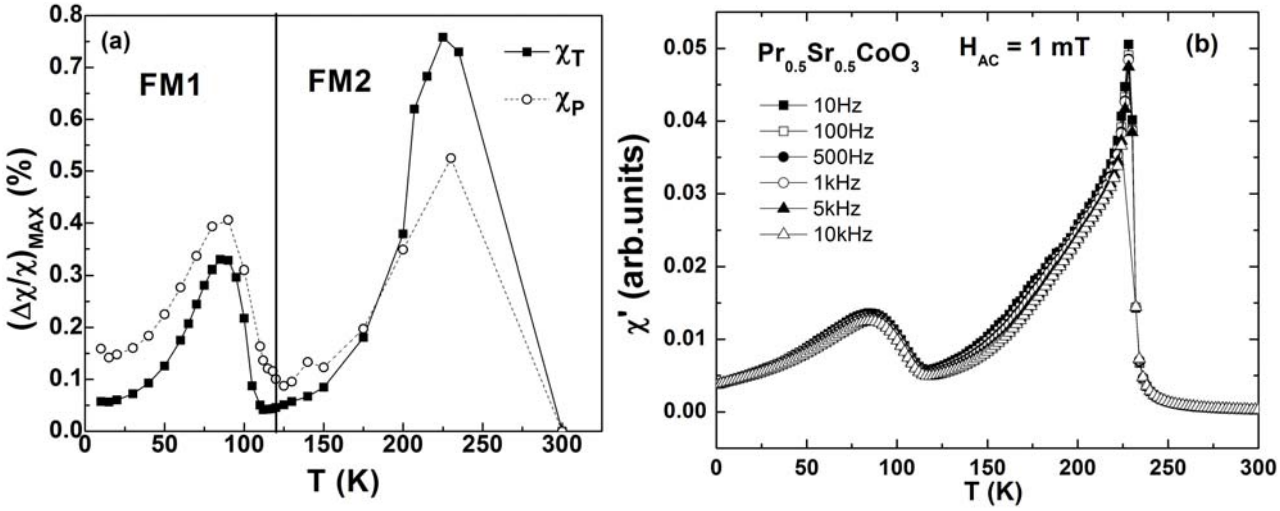
(a)
FM1
FM2
χ_T
χ_P
$(\Delta\chi/\chi)_{MAX}$ (%)
T (K)
$Pr_{0.5}Sr_{0.5}CoO_3$
H_{AC} = 1 mT
(b)
10Hz
100Hz
500Hz
1kHz
5kHz
10kHz
χ' (arb.units)
T (K)

Figure 6.